

Site Resonance Observed At Yan-Liau Station in Hualien, Taiwan

HUEY-CHU HUANG^{1,2}, and HUNG-CHIE CHIU²

(Manuscript received 18 October 1992, in final form 17 February 1993)

ABSTRACT

An earthquake which registered magnitude 6.9 on the Richter scale occurred on 13 December 1990 in the south of Hualien. A temporary array which consisted of 15 triaxial digital accelerographs had been deployed in the epicentral area so as to monitor aftershocks. Roughly 600 earthquakes triggered this array during the deployment of three months and 162 of them were detected at Yan-Liau, one station of this temporary array. Most of its accelerograms have exhibited evident resonance phenomenon. Polarization analyses of 30 well-recorded accelerograms have been conducted in this paper so as to examine the resonance effect. The predominant frequencies of P waves have been indicated by the results to have a wide range of distributions which span from 8 to 18 Hz, while most of the S waves and their following resonance waves fell in a narrow frequency band between 7 and 8 Hz. Although resonance phenomenon is significant at Yan-Liau, the resonance waves do not polarize in a preferred orientation and no particular connections have been found among the polarization directions of the P, direct S and resonance waves.

1. INTRODUCTION

The site effect has been documented by many researchers to be an important factor which may significantly modify the recorded ground motions. The influence of the site on the ground motions is a complicated effect. It appears in different ways and is dependent on the types of quantities in consideration (*e.g.* response spectra, ground acceleration, velocity and displacement, Fourier spectra,...., etc.) and the parameters selected for classifying the site effects (*e.g.* geological conditions, types of input waves, topography, subsurface structure, weak or strong motion, the incident angles of input wave). For example, four types of site conditions have been used by Seed *et al.* (1976) in examining the site-dependent response spectra. The site conditions have been included in the regression analysis of Fourier spectra by Trifunac (1976). The responses of flat surface layer for incident P, SV and SH waves

¹ Institute of Geophysics, National Central University, Chung-Li, Taiwan, R.O.C.

² Institute of Earth Sciences, Academia Sinica, Nankang, Taiwan, R.O.C.

in various incident angles have been calculated by Burrige *et al.* (1980). A great variety of numerical methods have been used in calculation of the site response in the presence of irregular topography (*e.g.* Boore, 1972; Bouchon 1973; Wong and Jennings, 1975; Bard, 1982; Sanches-Sesma, 1985; Chiu and Huang, 1992), sediment-filled valley (Wong and Trifunac, 1974), and alluvium (Chiu *et al.*, 1991). The resonance is one of the most important site effects. Whether a particular site has a preferable direction of ground motion in a given frequency range is an interesting topic of research for earthquake engineers. A dramatic example of resonance is the amplification of 2-sec energy caused by lakebed deposits in Mexico City during the 1985 Michoacan earthquake (Campillo *et al.*, 1989; Kawase and Aki, 1989). A sediment-filled valley which has been indicated in a numerical work of Bard and Bouchon(1985) begins to vibrate with a single frequency when the shape ratio (thickness/width) exceeds a certain value. A similar phenomenon has been found in a semi-cylindrical canyon (Trifunac, 1971). A soft surface layer in the deep basin has been introduced by Kawase and Aki (1989) and they successfully explained the long duration observed at station CDAO in Mexico City during the 1985 Michoacan earthquake.

The records of 10 October 1987 mainshock and its aftershocks in Whittier Narrows, California, were analyzed by Vidale *et al.* (1991). Among 11 strong-motion stations, 8 of them were shown to have a similar polarization, which were expected to be different due to the different seismic source mechanisms. Also, the shear-wave polarization from the 10 aftershocks of Loma Prieta earthquakes were shown to have a strong azimuthal dependence by Bonamassa and Vidale (1991).

Most of the accelerograms recorded at Yan-Liau have an evident resonance phenomenon (a single-frequency oscillation). The characteristics of resonance has been investigated in this paper by using the particle motion and the polarization analysis. Three windowed seismic traces which correspond to the P, S and resonance waves after the S-arrival are selected for these analyses. Each windowed seismic trace has been transformed to frequency domain, filtered by a band-pass filter with a 2-Hz cosine taper centered at each frequency, then transformed back to time domain for polarization analysis. A total of 30 well-recorded earthquakes are selected in this study.

2. THEORY OF COMPLEX POLARIZATION ANALYSIS

The polarization analysis used in this paper has followed the approach given by Vidale (1986). For a given three-component accelerogram, we can construct the analytic signals and covariance matrix to reduce the analysis to be an eigenvalue problem.

Although eigenvalues and eigenvectors can be obtained at each time step, the results become more significant if the covariance matrix is constructed with a finite length in analytic signal.

The eigenvector (x_0, y_0, z_0) associated with the largest eigenvalue λ_0 points in the direction of the largest amount of polarization. However, the phase in the complex plane of the eigenvectors is initially arbitrary; the maximum value on the complex plane needs to be determined. First, the eigenvector is normalized to have length 1. The eigenvector associated with the largest eigenvalue is then rotated between 0° and 180° so as to find the maximum length of the real component of the eigenvector X , where

$$X = \sqrt{(Re(x_0 cis\alpha))^2 + (Re(y_0 cis\alpha))^2 + (Re(z_0 cis\alpha))^2} \quad (1)$$

and $cis\alpha$ is $\cos\alpha + isin\alpha$ and $Re(x)$ is the real part of x . The vector (x_0, y_0, z_0) is then rotated by the angle α , and the elliptical component of polarization may be estimated by

$$P_E = \frac{\sqrt{1 - X^2}}{X} \quad (2)$$

Since the eigenvector is normalized, $\sqrt{1 - X^2}$ is the length of the imaginary part of the eigenvector, and P_E is the ratio of the imaginary part of the eigenvector to the real part of the eigenvector. P_E is 1 for circularly polarized motion, but P_E is 0 for linearly polarized motion.

The strike of the direction of maximum polarization is

$$\phi = \tan^{-1} \left(\frac{Re(y_0)}{Re(x_0)} \right) \quad (3)$$

The dip of the direction of maximum polarization is

$$\delta = \tan^{-1} \left(\frac{Re(z_0)}{\sqrt{(Re(x_0))^2 + (Re(y_0))^2}} \right) \quad (4)$$

In this paper, the strike and dip defined in equations (3) and (4) range from -90° to 90° , where 0° strike and dip represent a vector which points horizontally in the direction back to the epicenter.

The eigenvectors associated with the intermediate eigenvalue λ_1 and smallest eigenvalue λ_2 respectively point in the directions of the intermediate and least amount of polarization. The eigenvectors corresponding to λ_0 , λ_1 , and λ_2 are orthogonal. The degree of linear polarization can be defined as (Samson and Olson, 1980)

$$P_S^2 = \frac{(\lambda_0 - \lambda_1)^2 + (\lambda_1 - \lambda_2)^2 + (\lambda_2 - \lambda_0)^2}{2(\lambda_0 + \lambda_1 + \lambda_2)^2} \quad (5)$$

P_S is near 1 when the signal is totally polarized, and P_S decreases to 0 when it is unpolarized.

3. DATA ANALYSES AND DISCUSSIONS

Four days after the 13 December 1990 Hualien, Taiwan earthquake, a temporary array which consisted of 15 triaxial digital accelerographs was deployed in the epicentral area to monitor aftershocks. The locations of 15 temporary stations (with station number greater than 60) and several SMART-2 stations are shown in Figure 1. The Yan-Liau station was named S63. During the deployment of three months, roughly 600 earthquakes triggered this array and 162 (both open and solid circles in Figure 2) of them were detected by Yan-Liau station. Among these earthquakes, 30 well-recorded accelerograms with simple waveforms were selected for this study. The criterion of simple waveform can exclude these records which may have been strongly affected by the source effect. These events are marked by solid circles in Figure 2. They cover a magnitude range from 3.2 to 5.3 and most of their epicentral distances are less than 18 km and focal depths are less than 10 km (Figure 2 and Table 1).

Evidences show that the resonance observed at Yan-Liau is caused by the site effect. Some selected north-south component seismograms for event 90121756 are shown in Figure 3. From a comparison of the time histories of these records, the resonance of waveform at

S63 is remarkable. The Fourier spectra corresponding to the accelerograms in Figure 3 are shown in Figure 4. A single-frequency oscillation (near 7.6 Hz) only exists at Yan-Liau and does not appear in other stations. If this single-frequency oscillation is due to the source effect, the same frequency signal should appear in other stations. However, in Figure 3 and Figure 4, no indications have shown that this single-frequency oscillation is related to the source effect. Furthermore, besides the selected 30 records, the same oscillation can be found at the rest of records at Yan-Liau. Based on this evidence, we exclude the possibility that this resonance is due to the source effect. The seismograms and Fourier spectra at Yan-Liau from different earthquakes are shown in Figure 5 and 6. The resonance always exists, no matter what the azimuth and hypocenter distance of these earthquakes are. All spectra have a simple shape and a predominant frequency which is concentrated near 7 and 8 Hz. This fact also excludes the possibility that ray-path effects may create the resonance waves.

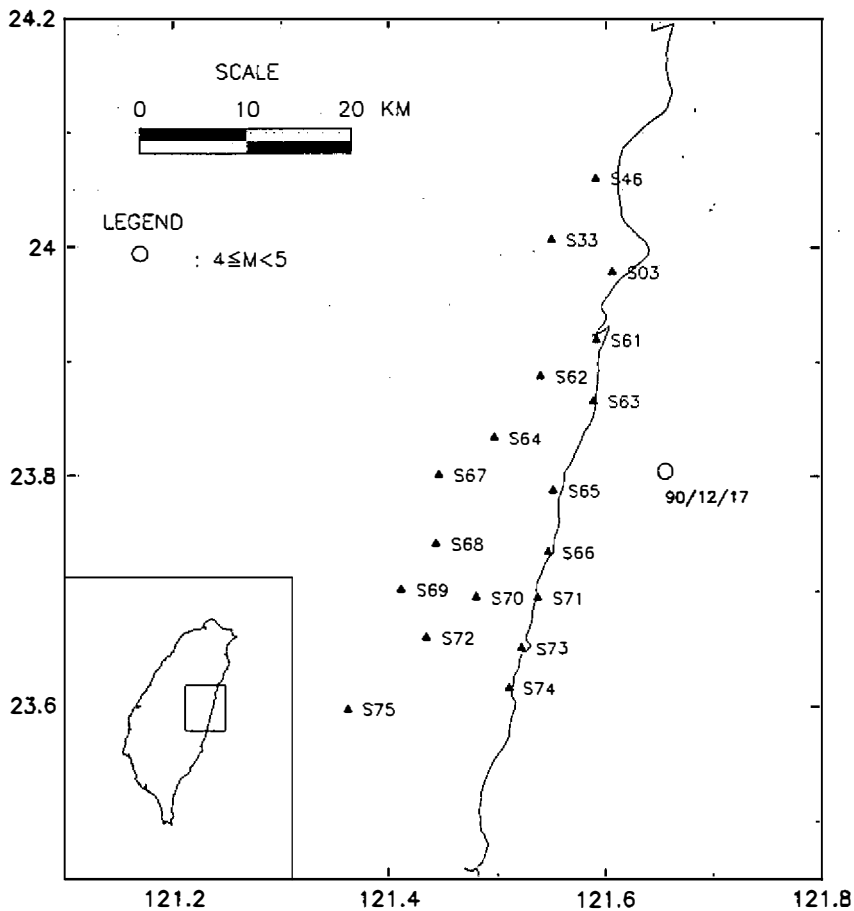


Fig. 1. Location of some selected SMART2 stations and stations of the temporary array (station number greater than 60). Open circle marks the epicenter of event 90121756.

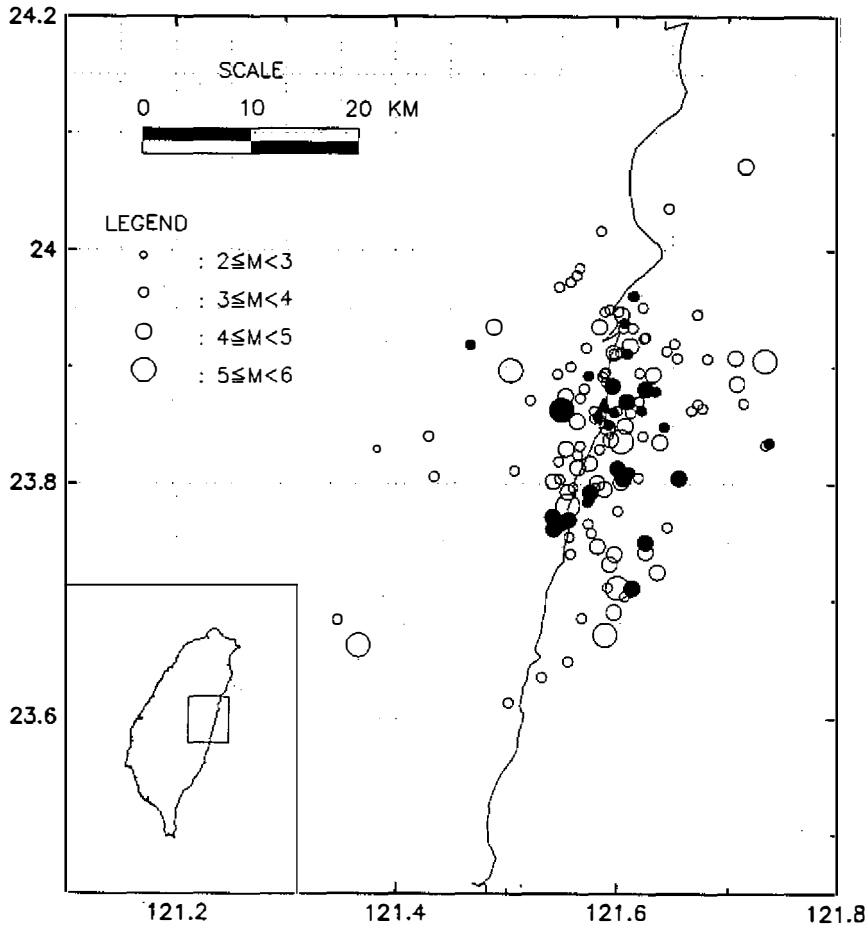


Fig. 2. Epicenters of 162 earthquakes triggered the strong-motion accelerograph at Yan-Liau station, 30 (solid circles) of them with simple waveform were selected for this study.

The poor coupling and malfunction of sensor or recorder are doubtfully related to the resonances. Some evidences show that the resonance waves observed at Yan-Liau do not belong to these cases. If the coupling may be poor during the strong shaking (event 91012006 which has PGA of 150.59 cm/sec^2), it should not be a problem during the small shaking such as events 90121760 and 90122042 (Figure 5). The malfunction of sensor or recorder may result in a single-frequency oscillation for all events and entire records. But the difference of the frequency contents among various earthquakes and a large difference of frequency content between P and S waves still can be found in the observed data. Furthermore, several instrument calibrations were conducted here during the three-month deployment and the instruments were indicated by all calibrations to be in good condition. This single-frequency oscillation primarily coming from site effect can be stated here with strong confidence based on these facts.

Table 1. Earthquakes used in this analysis.

Event No	Record Id	Latitude (degree)	Longitude (degree)	ML	Epi Dist (Km)	Depth (Km)
1	9012162863	23.86	121.60	3.47	1.05	3.05
2	9012165363	23.81	121.61	3.83	6.63	0.55
3	9012175563	23.69	120.94	3.20	69.40	2.62
4	9012175663	23.81	121.66	4.02	9.59	1.87
5	9012176063	23.83	121.74	3.82	15.64	2.09
6	9012176863	23.81	121.60	4.04	5.96	1.31
7	9012180363	23.89	121.57	3.35	3.25	11.45
8	9012186763	23.85	121.59	3.71	1.51	1.47
9	9012187463	23.79	121.58	4.52	8.20	3.28
10	9012199963	23.86	121.58	3.45	1.11	3.62
11	901219C863	23.78	121.57	3.88	9.14	0.47
13	9012204163	23.77	121.54	4.27	11.43	0.57
14	9012204263	23.71	121.61	4.14	17.36	6.07
15	9012204363	23.76	121.54	4.45	12.43	2.80
16	9012204763	23.77	121.56	4.10	11.17	3.37
17	9012210763	23.85	121.59	3.75	1.74	0.35
18	9012231463	23.94	121.61	3.99	8.20	0.11
19	9012232363	23.91	121.61	3.62	5.49	0.80
20	9012250263	23.92	121.47	3.44	13.56	2.65
21	9012250363	23.86	121.62	3.31	3.44	0.66
22	9012251163	23.75	121.63	4.91	13.37	4.20
23	9012280763	23.85	121.64	3.75	5.83	0.12
24	9101080363	23.96	121.61	3.78	10.88	3.41
25	9101090763	23.81	121.60	4.07	6.48	1.47
26	9101120263	23.88	121.63	4.23	4.18	0.44
27	9101170163	23.88	121.63	3.98	4.97	5.82
28	9101200663	23.86	121.55	5.25	3.90	24.16
29	9102180163	23.80	121.61	4.47	7.00	0.37
30	9102190163	23.87	121.61	4.47	2.18	0.83

Particle-motion analysis can be used to examine the characteristics of resonance. It gives the direction and ellipticity of polarization of resonance waves. Figure 7 is an example of particle-motion analysis for the two horizontal components of accelerograms with resonance (top) and without resonance (bottom). Both records came from the same event (90121756). The top one was recorded at S63 (Yan-Liau) and the bottom one at S65. The time interval for each particle-motion circle is 0.4 sec. The starting time and maximum amplitude for each particle-motion circle are shown on the top of each circle. At Yan-Liau, it starts with linear polarization at the arrival of primary S waves. After the primary S waves, most trajectories of particle motion are elliptic and clockwise from 11.4 to 13.0 sec and the axes of ellipses

change their orientations and ellipticity from time to time. On the other hand, the unresonance waves at S65 demonstrated very random particle motions. Although the plots of particle-motion circles are more intuitive than the results of other methods, particle-motion analysis

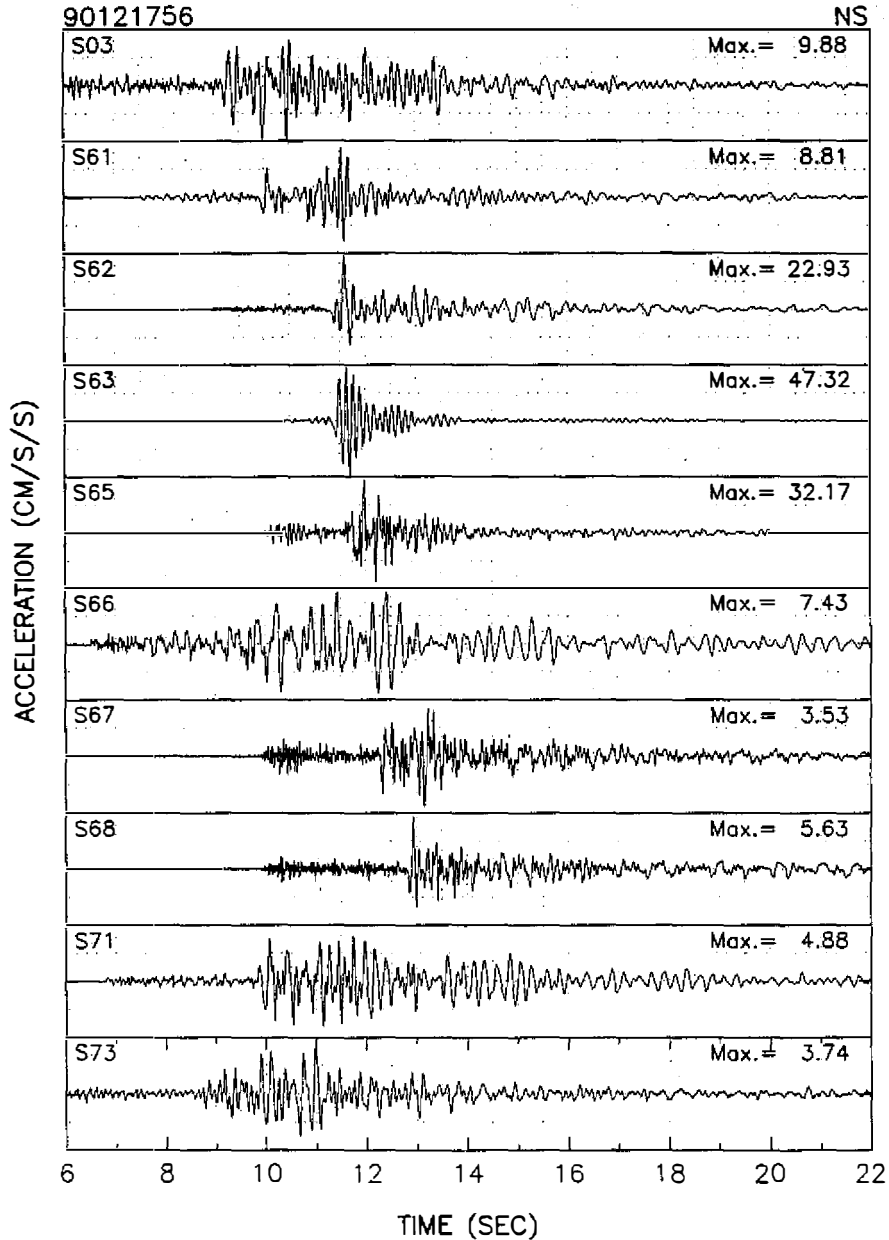


Fig. 3. Selected NS-component accelerograms recorded in event 90121756. The station code is given in the upper-left of each plot and the peak acceleration is shown in upper-right corner.

finds it rather difficult in displaying the time-dependent characteristics of polarization. A more concise and complete analysis is the polarization analysis as described in the previous section. This analysis provides the time-dependent strikes and dips of polarization axes, the strength of polarization and the ellipticity of the polarization. The same records used in particle-motion analysis, shown in Figure 7, are also used to demonstrate polarization analysis. The summary of this analysis is given in Figure 8. The left side of Figure 8 is the

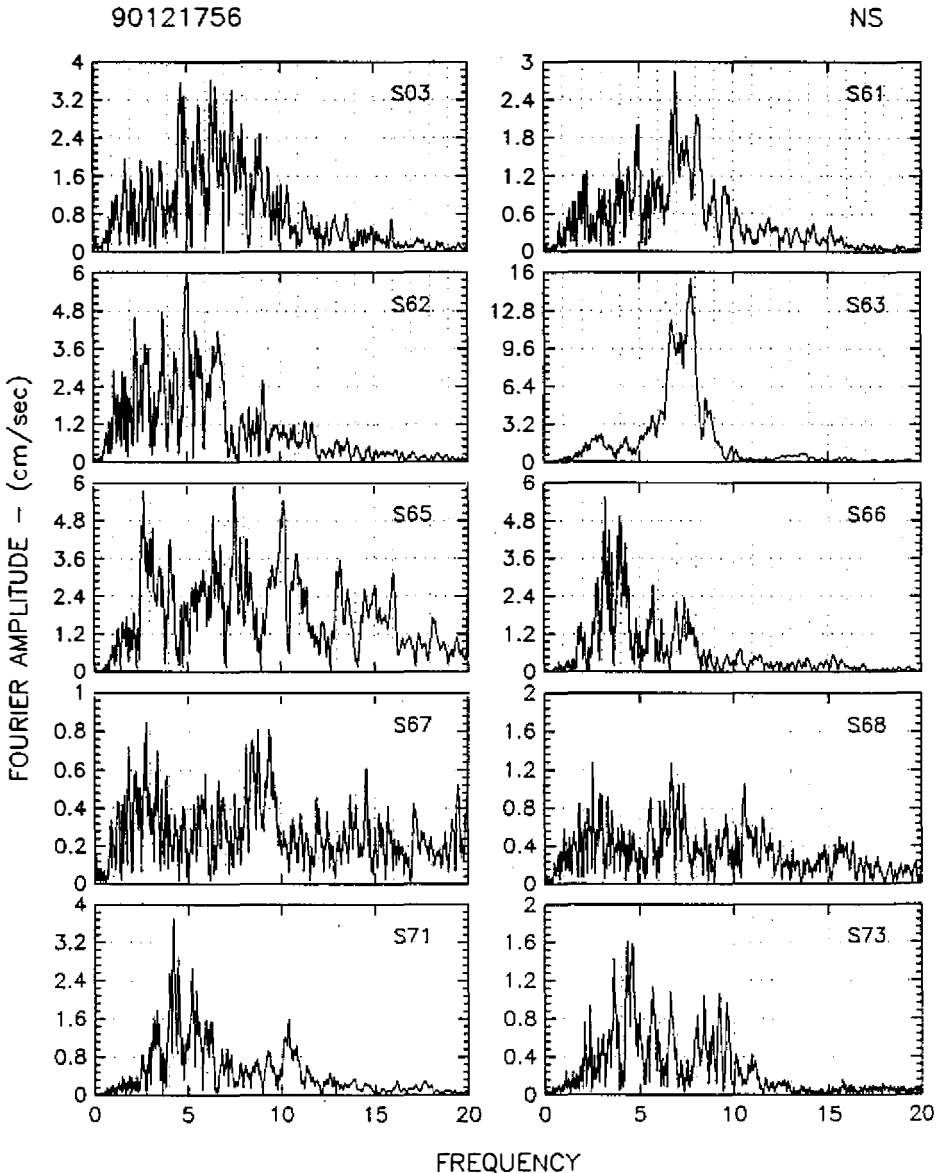


Fig. 4. The Fourier spectra corresponding to the accelerograms in Figure 3.

result at Yan-Liau station. From the top to the bottom are three-component accelerations: the strike of major axis, the dip of major axis, the strength of polarization and ellipticity of polarization ellipse. The change of strike before S-wave arrival (*e.g.*, background noise and P wave) is very fast and random. During the strong shaking (11.3 to 12.7 sec), the direction

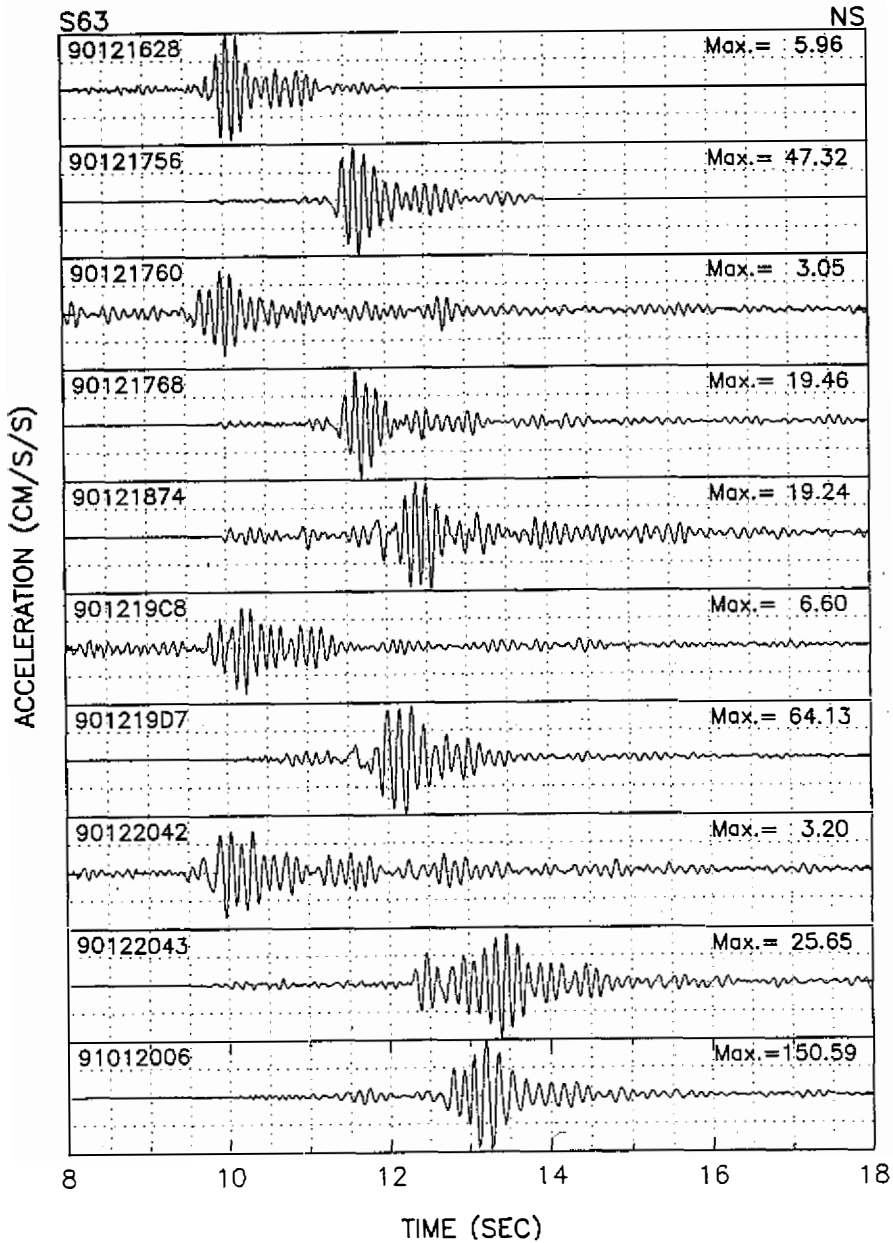


Fig. 5. Selected NS-component accelerograms recorded at Yan-Liau (S63). The first 8-digit number in the upper-left of each plot is the event ID of accelerogram.

of strike changes from NE-SW direction to NW-SE direction. An interesting result is that the major axis of first-S wave almost coincides with the direction estimated from azimuth between the epicenter and Yan-Liau station. Before the S-wave arrival, ground motions were dominated by vertical component, therefore, dips are very close to $\pm 90^\circ$. Dips are also random before the P-wave arrival and become very close to 0° during the strong shaking, because of the strong polarization in the horizontal motions. Most of P_S values are very

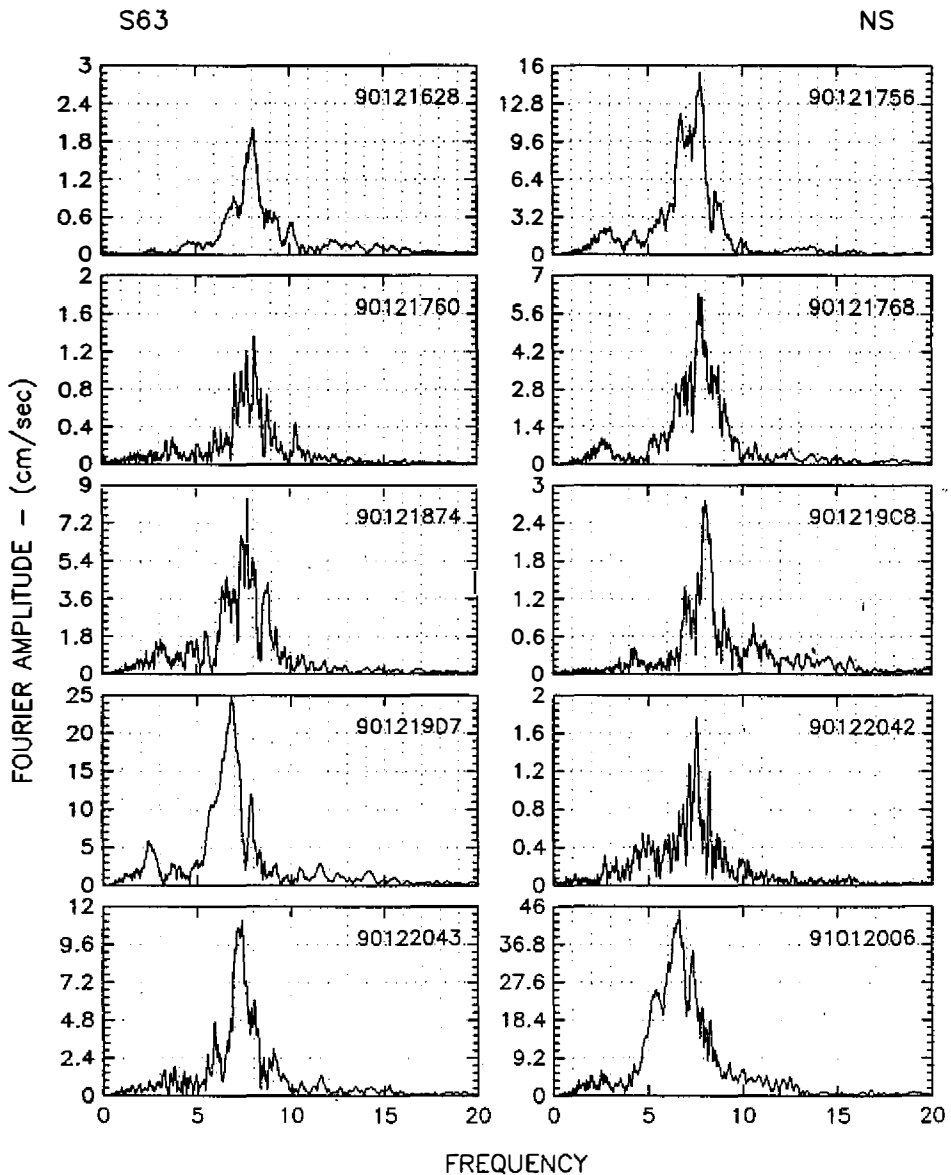


Fig. 6. The Fourier spectra corresponding to the accelerogram in Figure 5.

close to 1 between P arrival and the end of strong shaking which implied that the polarization is primary in the major axis and small in the rest two axes. Starting from 11.2 sec, P_E value increases from 0 to 0.9 at 11.7 sec and back to 0 at 12.5 sec. The changes of P_E show that the polarization starts with linear polarization ($P_E = 0$) and turns to be a circular polarization ($P_E = 1$) and finally goes back to linear polarization. This phenomenon is the same as what has been previously seen here in particle-motion analysis (Figure 7). The right side of Figure 8 is the result of the same analysis at station S65. The significant difference between the right and left side of Figure 8 is P_S . P_S at S63 is almost equal to 1 during the strong shaking, but P_S at S65 is near 0.5 for the unresonance waves. In general, for unresonance wave, the degree of polarization is small.

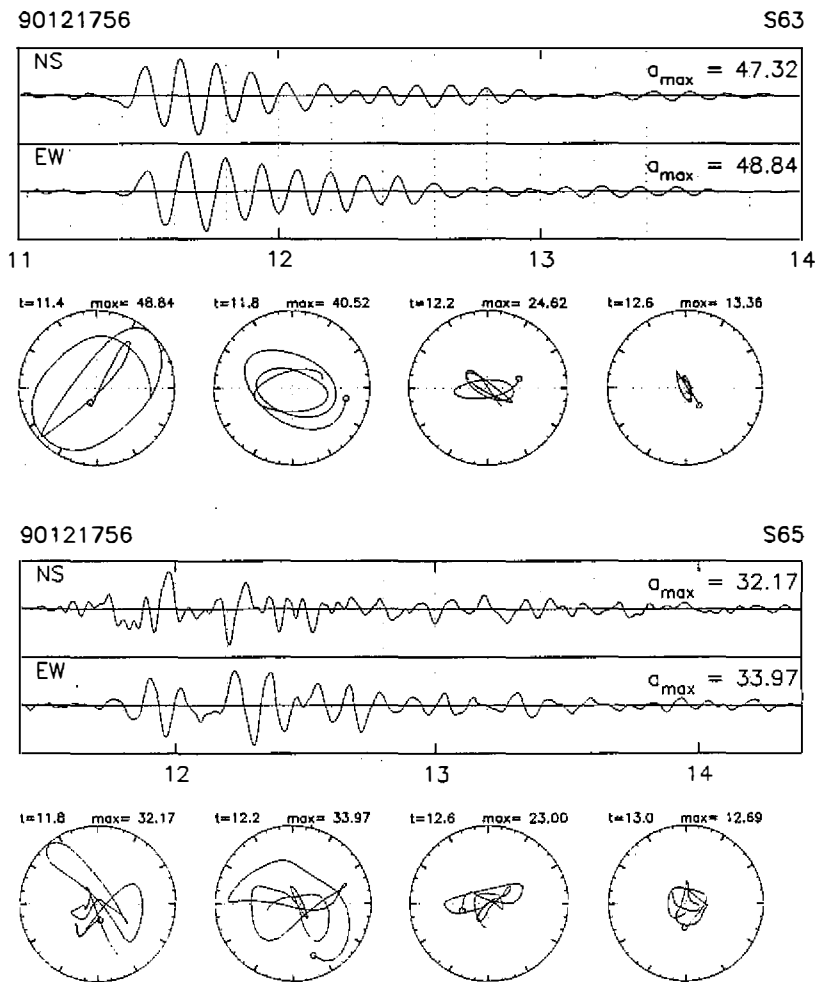


Fig. 7. Particle-motion diagrams for the two horizontal components of accelerograms recorded at S63 (Yan-Liau) and S65 in event 90121756. The starting time and the maximum amplitude in each diagram are shown in the top of each particle-motion circle.

In order to investigate the directional site resonances and determine their consistency and strength, a systematic estimate of polarization direction is performed at different frequencies and time windows for these earthquakes (Table 1). The time windows include 0.5 sec for P wave, 1 sec for S wave, and 5 sec for the resonance waves following the S wave. In the frequency domain, we divide signals into 20 bands centered from 1 to 20 Hz by using a 2 Hz-cosine taper.

The P-wave polarization direction versus frequency for the 30 events is shown in Figure 9. For each event, the three-component accelerations were divided into 20 frequency bands and the associated P wave was extracted for polarization analysis to determine the strength and strike of the maximum polarization. The size of symbols represents the relative energy distribution at different frequencies in the same earthquake. The amplitudes of 20 frequency

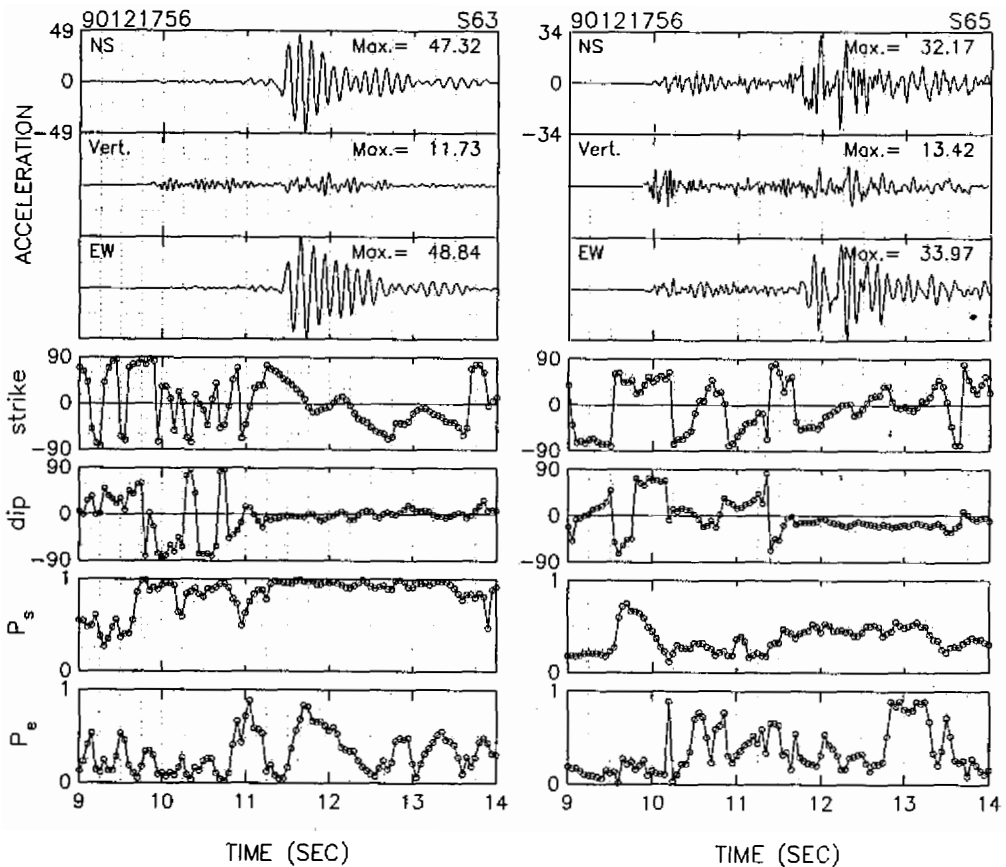


Fig. 8. Example of polarization analysis of event 90121756 at S63 (Yan-Liau) and S65. From the top to the bottom are the three-component traces, strike and dip of major polarization axes, the strength (P_S) of polarization and the ellipticity (P_E) of polarization ellipse.

bands have been normalized by its maximum value. The polarization directions for each frequency band are not necessarily the same. For P wave, the major polarization directions (thick-line square in Figure 9) have a quite diverse distribution both in frequency (8 - 18 Hz) and polarization directions (-75° - 50°). The polarization of S (Figure 10) and resonance waves (Figure 11) are shown in a comparison with P wave to be confined in a more narrow frequency band (7 - 8 Hz); the polarization directions, however, have a very diverse distribution which covers almost all directions. For the resonance waves, five events shift away from the centered frequency (7 - 8Hz); one event shifts its frequency to 6 Hz and four events shift to higher frequencies (9 and 10 Hz). 13 events can be seen here from a careful examination of Figure 11 to have a preferable direction of polarization and fall between -10° and -35° . In order to further investigate the properties of these events, the major polarization directions of P, S and resonance waves of these events are plotted together in Figure 12. As shown in the figure, no particular connections have been found among the polarization directions of P, S and resonance waves.

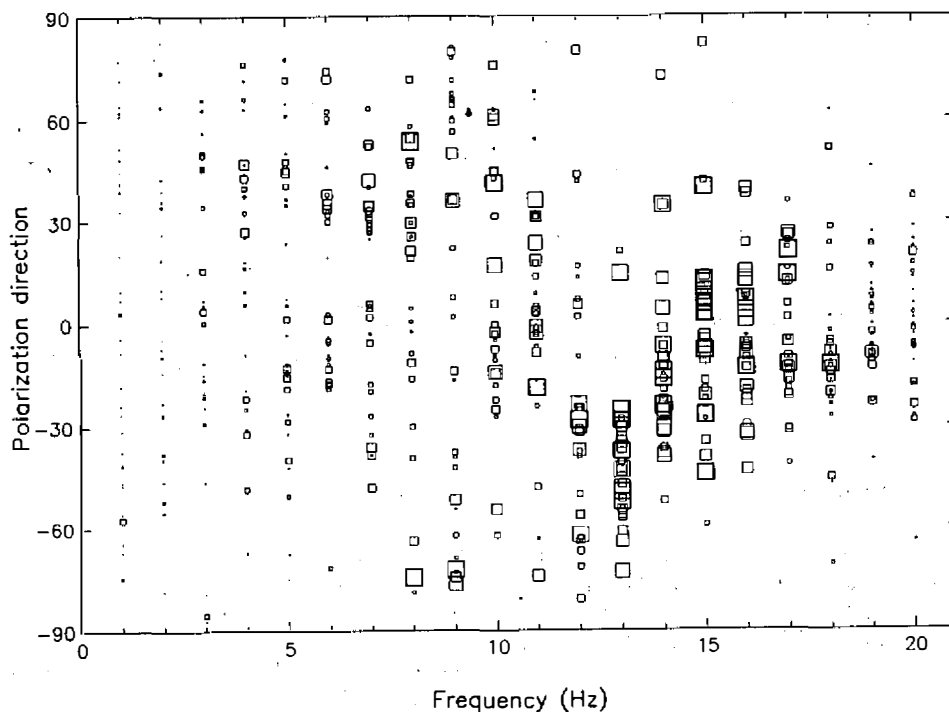


Fig. 9. Frequency-dependent polarization direction of P waves. The signals of 20 frequency bands at each Hertz from 1 to 20 Hz were subtracted for analysis. The size of the square represents the relative amplitude among the 20 frequency bands. A total of 30 earthquakes are listed in Table 1 and are included in this plot.

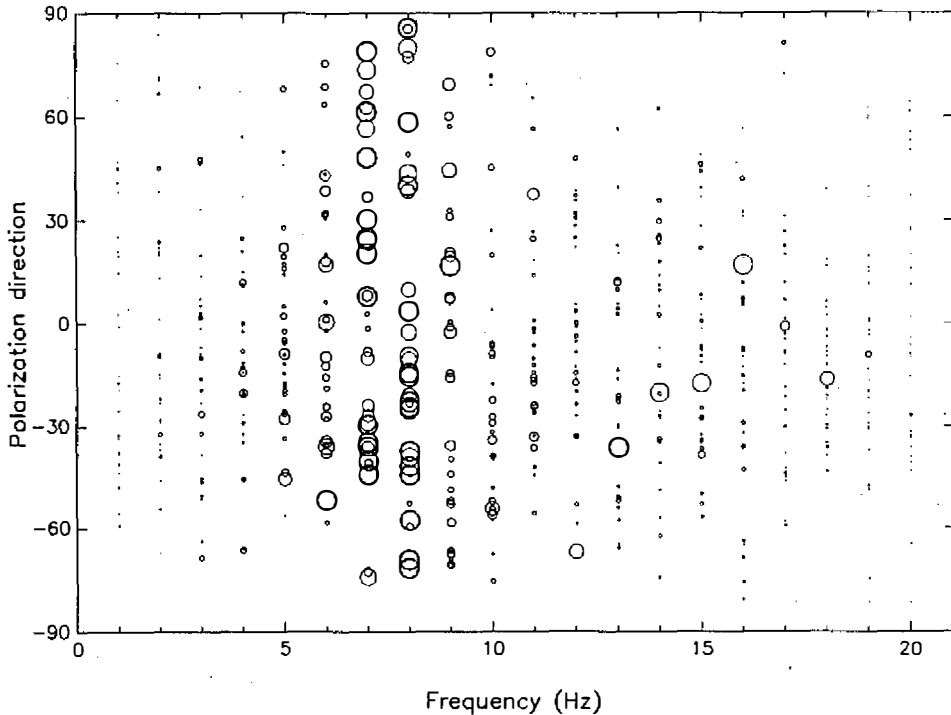


Fig. 10. Frequency-dependent polarization direction of direct S (S_1) waves. The earthquakes used here is same as that in P-wave analysis.

4. CONCLUSION

The resonance phenomenon found at Yan-Liau station after an examination of the accelerograms and their Fourier spectra is neither caused by the source nor path effect. The possibility that resonance comes from the malfunction of instruments and poor coupling between ground and instrument was also very low. Therefore, the best explanation concluded here was that the resonance occurred due to the site effect. In a systematic analysis of 30 events, the resonance observed at Yan-Liau was found to have occurred in a narrow frequency band between 7 and 8 Hz. This resonance frequency was similar to that of the direct S wave, but it was quite different from that of P wave which exhibited a rather diverse distribution in predominant frequencies. Among 30 events, the resonance waves of 13 events had similar polarization directions, although the corresponding polarizations of P and direct S waves had very diverse distribution of polarization directions. The others, however, did not show a preferable polarization direction. It seems that the directional resonance does not exist at Yan-Liau.

Acknowledgments This research was supported by the Academia Sinica and the National Science Council under contract NSC-81-0202-M001-03. The support of these organizations is gratefully acknowledged.

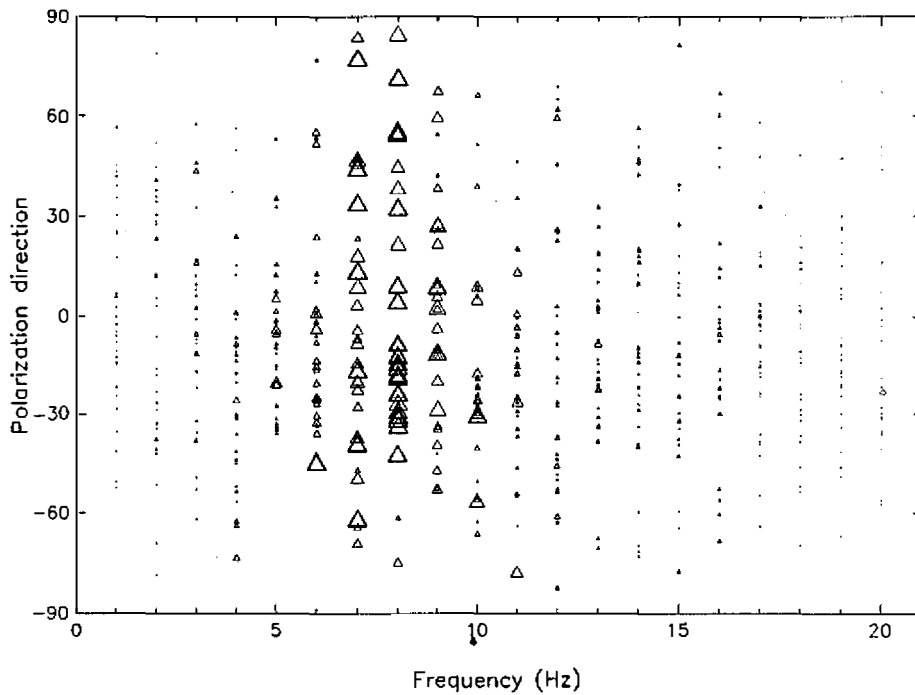


Fig. 11. Frequency-dependent polarization direction of resonance waves (S_2). The earthquakes used here is same as that in P-wave analysis.

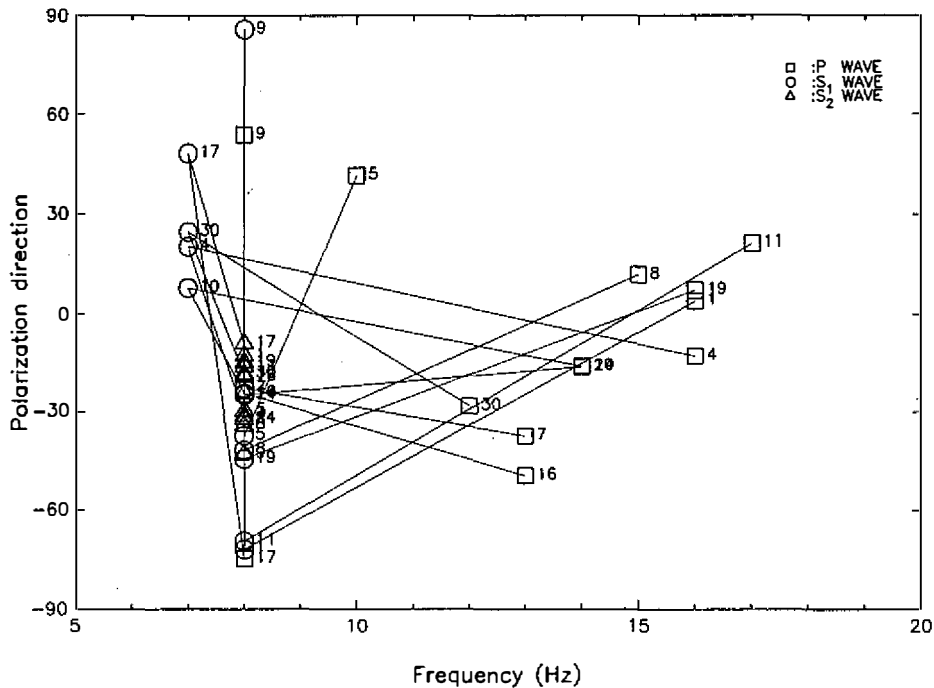


Fig. 12. Relationships of Polarization direction of resonance waves of 13 earthquakes.

REFERENCES

- Bard, P. Y. (1982). Diffracted waves and displacement field over two dimensional elevated topographies, *Geophys. J. R. Astr. Soc.*, **71**, 731-760.
- Bard, P. Y. and M. Bouchon (1985). The two-dimensional response of sediment-filled valleys, *Bull. Seism. Soc. Am.*, **75**, 519-541.
- Bonamassa, O. and J. E. Vidale (1991). Directional site resonances observed from aftershocks of the 18 October 1989 Loma Prieta earthquake, *Bull. Seism. Soc. Am.*, **81**, 1945-1957.
- Boor, D. M. (1972). A note on the effect of simple topography on seismic SH waves, *Bull. Seism. Soc. Am.*, **62**, 275-284.
- Bouchon, M. (1973). Effect of topography on surface motion, *Bull. Seism. Soc. Am.*, **63**, 615-632.
- Burridge, R., F. Mainardi, and G. Servizi (1980). Soil amplification of plane seismic waves. *Phys. Earth Planet. Int.*, **22**, 122-136.
- Campillo, M., J. C. Gariel, K. Aki, and F. J. Sanchez-Sesma (1989). Destructive strong ground motion in Mexico City: source, path and site effects during the great 1985 Michoacan earthquake, *Bull. Seism. Soc. Am.*, **79**, 1718-1734.
- Chiu H. C., T. L. Teng, and H. L. Wong (1991). Scattering effects of SH waves due to an irregular structure: a case at the SMART1 array site, *Proceedings of the Geological Society of China.*, **34**, 91-110.
- Chiu H. C., and H. C. Huang (1992). Effects of the Canyon topography on ground motions at the Feitsui Damsite, *Bull. Seism. Soc. Am.*, **82**, 1646-1660.
- Kawase, H. and K. Aki (1989). A study on the response of a soft basin for incident S, P, and Rayleigh waves with special reference to the long duration observed in Mexico City, *Bull. Seism. Soc. Am.*, **79**, 1361-1382.
- Samson, J.C. and J.V. Olson (1980). Some comments on the descriptions of the polarization states of waves, *Geophys. J. R. Astr. Soc.*, **61**, 115-129.
- Sanchez-Sesma, F. J. (1985). Diffraction of elastic SH waves by wedges, *Bull. Seism. Soc. Am.*, **75**, 1435-1446.
- Seed, H. B., C. Ugas, and J. Lysmer (1976). Site-dependent spectra for earthquake-resistant design, *Bull. Seism. Soc. Am.*, **66**, 221-244.
- Trifunac, M. D. (1971). Surface motion of a semi-cylindrical alluvial valley for incident plane SH waves, *Bull. Seism. Soc. Am.*, **61**, 1755-1770.
- Trifunac, M. D. (1976). Preliminary empirical model for scaling Fourier amplitude spectra of strong ground acceleration in terms of earthquake magnitude, source-to-station distance and recording site condition, *Bull. Seism. Soc. Am.*, **66**, 1343-1373.
- Vidale J. E. (1986). Complex polarization analysis of particle motion, *Bull. Seism. Soc. Am.*, **76**, 1393-1406.
- Vidale, J.E., O. Bonamassa, and H. Houston (1991). Directional site resonances observed from the 1 October 1987 Whittier Narrows, California, earthquake and the 4 October aftershock, *Earthquake Spectra*, **7**, 107-125.
- Wong, H. L., and M. D. Trifunac (1974). Scattering of plane SH waves by a semi-elliptical canyon, *Int. J. Earthquake Eng. Structr. Dyn.*, **3**, 157-169.
- Wong, H. L., and P. C. Jennings (1975). Effect of Canyon topography on strong ground motion, *Bull. Seism. Soc. Am.*, **65**, 1239-1257